RETINAL NERVE FIBER LAYER ANALYSIS VIA MARKOV RANDOM FIELDS TEXTURE MODELLING

Jan Odstrčilík, Radim Kolář, Vratislav Harabiš, Jiří Gazárek and Jiří Jan

Department of Biomedical Engineering, FEEC, Brno University of Technology
Kolejni 4, 612 00 Brno, Czech Republic
phone: + (420) 541 149 541, email: xodstr02@stud.feec.vutbr.cz
web: www.dbme.feec.vutbr.cz

ABSTRACT

The texture analysis of the retinal nerve fiber layer (RNFL) in colour fundus images is a promising tool for early glaucoma diagnosis. This paper describes model-based method for detection of changes in the RNFL. The method utilizes Gaussian Markov random fields (GMRF) and the least-square error (LSE) estimate for the local RNFL texture modelling. The model parameters are used as a texture features and non-linear classifier based on the Bayesian rule is used for classification of healthy and glaucomatous RNFL tissue. The proposed features are tested in the sense of classification errors and also they are applied for segmentation of RNFL defects in a high-resolution colour fundus-camera images. The results are also compared with the Optical Coherence Tomography images regarded as a gold standard for our application due to the possibility of quantitative RNFL thickness measurement.

1. INTRODUCTION

Glaucoma is one of the most common causes of blindness with an average occurrence of 4.2% for ages above 60 years [15]. Glaucoma is characterized by retinal changes, particularly in the region of the optic nerve head (ONH): an enlargement of the ONH excavation, ONH hemorrhages, thinning of the neuroretinal rim, asymmetry of the cup between left and right eye, and progressive retinal nerve fiber layer (RNFL) atrophy. This RNFL loss can be relatively well indicated as a texture changes in fundus photographs (Figure 1). Early detection of the RNFL atrophy plays a crucial role in the effective treatment, because the retinal nerve fibers cannot be revitalized. Therefore, the analysis of retinal images has become an important issue in glaucoma diagnosis. The quantitative measurement of RNFL thickness with the Optical Coherence Tomography (OCT) is widely promoted by the ophthalmologists and a lot of papers concerning this modality have been already published, e.g. [3, 8, 14]. However the examination by OCT is still less available due to the high costs in many ophthalmology clinics all over the world. The main requirement in glaucoma diagnosis is an early detection of RNFL degeneration in order to set up the treatment as soon as possible. Hence, a mass screening program seems to be suitable for supporting the diagnosis. Well, an extensively available fundus-camera imaging can be offered for such a reasonable glaucoma screening.

There is a high effort to base the automated RNFL analysis on fundus-camera images since the 1980 [10], but until now, there is no routinely used method allowing automated RNFL diagnosis using only fundus camera images; although many contributions concerning this topic have been already published, e.g. [1, 2, 4, 6, 9, 17, 19].

Our contribution deals with a new model-based method utilizing Gaussian Markov random fields (GMRF) to model the local RNFL texture in high-resolution colour fundus-camera images. The model parameters are estimated by the least square error (LSE) approach and they are used as a texture classification features. Non-linear Bayesian classifier is used for discrimination between healthy and glaucomatous RNFL tissue. The classification performance is evaluated using cross-validation approach and also supervised machine learning is applied in order to detect RNFL loss in diagnostically important region in fundus images. The results are finally compared with the OCT data.

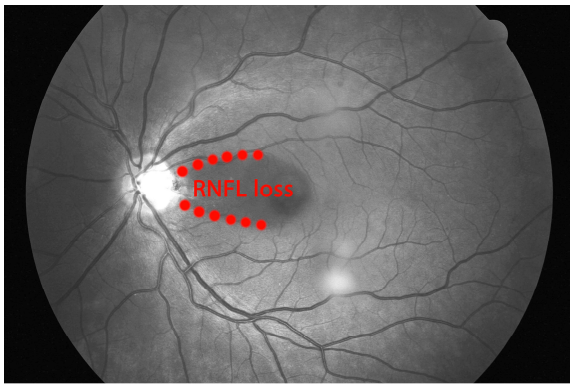

Figure 1 – Example of typical fundus image with distinctive RNFL loss; an average of green and blue channel of RGB colour image data is utilized.

2. EXPERIMENTAL DATA

Our retinal image database contains 18 images of healthy patients and 10 images of patients with glaucoma (RNFL defects). All images were acquired by digital fundus camera CANON CF-60UDi with 3504×2336 pixel resolution in RGB colour space and with 60° field of view. The JPEG image format with very low compression was applied. The proposed method utilizes only green and blue channel of RGB

 ISSN 2076-1465

image data (Figure 1). This is because the red channel does not contain any useful information about RNFL texture. Experimentally, it was found that an average of green and blue channel is the most relevant solution providing relatively good appearance of RNFL striation [16].

Using fundus camera images, the healthy RNFL tissue is characterized by lightly stripy textural appearance (Figure 2a), while RNFL defects appear with lack of such the lightly striation.

The method has been tested on manually selected square-shaped image regions with size 97 × 97 pixels from all retinal images included in the database. These image regions were divided into three classes (Figure 2b):

Class A - 141 image regions representing tissue with RNFL striations of glaucomatous patients;

Class B - 142 image regions representing tissue without RNFL striations of glaucomatous patients (RNFL loss);

Class C - 283 image regions representing RNFL striations of healthy patients (control group).

We have three classes of RNFL tissue, because we assume an eventual progression of the disease represented by class A as a sub step in degeneration of the nerve fibers.

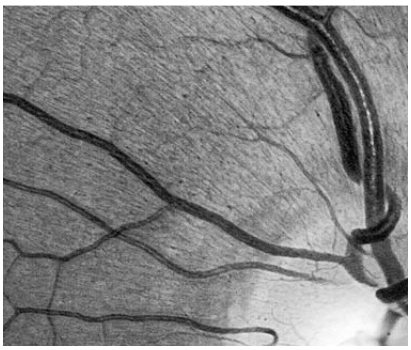

a)

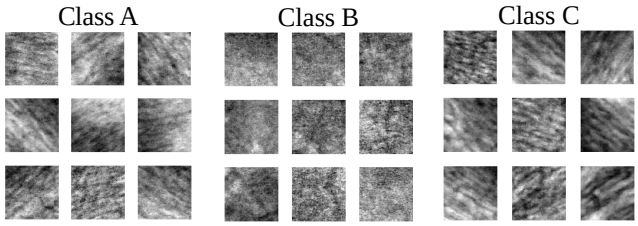

b)

Figure 2 – a) Example of the RNFL textural appearance, b) Example of randomly selected image regions according to the three classes of retinal tissue in the test dataset.

3. METHOD

3.1 Gaussian Markov random fields

Markov random fields texture modelling is an efficient tool enabling description of a probability of spatial interactions in a textural image so it has been extensively used in a lot of image processing applications, e.g. [18]. The detailed theory about Markov random field modelling in image analysis and texture classification can be found in [20].

Our paper introduces GMRF as a model of the RNFL providing textural features aimed to classify healthy and glaucomatous tissue in the fundus images.

The GMRF models an image texture *y(s)*, which is represented by a set of zero mean observations [18]:

$$y(s), s \in \Omega, \Omega = \{s = (i, j) : 0 \le i, j \le M - 1\}$$

for an $M \times M$ image lattice Ω. The GMRF model is a stationary non-causal two-dimensional autoregressive process assuming that the individual observations are governed by the following difference equation [18]:

$$y(s) = \sum_{r \in N_s} \phi_r y(s + r) + e(s),$$

where N_s is a neighborhood set centered at pixel s, ϕ_r is a model parameter of a particular neighbor r, and $e(s)$ is a stationary Gaussian noise process with zero mean and known variance σ:

$$E[e(s)] = 0,$$
$$E[e^2(s)] = \sigma.$$

A neighborhood structure depends directly on the order and the type of the model. We assume a fifth-order symmetric rotation-invariant neighborhood structure on rectangular lattice, as depicted in Figure 3.

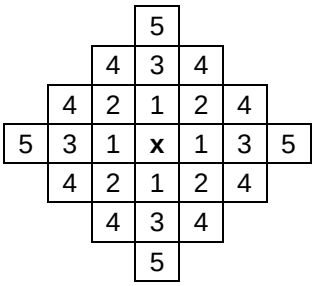

Figure 3 – Fifth-order symmetric rotation-invariant neighborhood.

According to this we have 6 parameters (texture features): five parameters describe influence of the neighbors to the central pixel and one Gaussian parameter σ describes model noise variance. These 6 features can be estimated in the least square error (LSE) sense [18]. The parameters are estimated by following equations:

$$\phi = \left[\sum_{\Omega} q(s) q^T(s) \right]^{-1} \left(\sum_{\Omega} q(s) y(s) \right),$$

$$\sigma = \frac{1}{M^2} \sum_{\Omega} (y(s) - \phi^T q(s))^2,$$

where

$$q(s) = col\left[\sum_{r \in N_i} y(s + r); i = 1, ..., I \right]$$

for an *I*th-order neighborhood.

3.2 Bayesian texture classification

The discrimination ability of proposed features has been tested by evaluation of the classification error using the Bayesian classifier.

Assume that we have a feature vector $x = [x_1, x_2, ..., x_D]$ of the dimension *D*. The probability that the feature vector belongs to a particular class ω_k can be referred to as a posterior probability and computed with the Bayes formula [13]:

$$P(\omega_k \mid x) = \frac{p(x \mid \omega_k) P(\omega_k)}{p(x)},$$

where $p(x \mid \omega_k)$ is a probability density function of class ω_k in the feature space and $P(\omega_k)$ is the a priori probability of the class ω_k before measuring any features. It can be estimated from the class proportions in the training set of supervised labelled data [13]. The probability $p(x)$ is only a scaling factor providing the sum of posterior probabilities is one. It can be computed by

$$p(x) = \sum_{i=1}^{K} p(x \mid \omega_i) P(\omega_i).$$

The proposed classifier assumes that the class-conditional probability density function $p(x \mid \omega_k)$ is modelled by Gaussians and thus describing a distribution of particular feature vectors in the feature space inside the particular class [13]. The Gaussian class model parameters can be estimated by several methods from the training dataset via supervised machine learning [13].

We use an iterative maximum-likelihood estimate with optimization technique based on modified expectation maximization algorithm (EM); see [13] for more details.

4. RESULTS AND DISCUSSION

4.1 Classification performance evaluation

The above described test dataset, consisting of three different classes of image regions representing the type of RNFL tissue, was used for training the classifier. The performance was evaluated for all particular combinations of classes (C-B, A-B, A-C, C-B-A). Six proposed features in the feature vector were sorted according to their relevance to target class in the sense of maximum relevance and minimum redundancy (MRMR) approach based on the evaluation of mutual information between particular features [5].

The repeated random sub-sampling cross-validation method was applied to test the classification accuracy. A 70% of randomly selected features from feature set were used for training, while remaining 30% was used for testing the proposed classifier. The training and testing procedure was run 100 times and the average classification error was computed. The results for particular combination of classes are shown in Table 1.

Table 1 – Classification errors in percents for all combinations of classes and features sorted according to their relevance; index *i* of the feature f_i represents an order in the feature vector.

Features selection	C – B	A – B	A – C	C – B – A
f_1	8.83 ± 2.53	9.13 ± 2.15	46.52 ± 5.06	37.13 ± 3.36
f_1-f_5	6.94 ± 2.81	7.17 ± 2.46	43.58 ± 4.81	34.10 ± 3.33
f_1-f_5-f_6	4.90 ± 2.11	7.08 ± 2.39	38.01 ± 4.90	30.25 ± 3.36
f_1-f_5-f_6-f_4	1.83 ± 1.62	5.92 ± 2.40	24.52 ± 4.23	20.26 ± 3.21
f_1-f_5-f_6-f_4-f_3	**0.55 ± 0.82**	4.99 ± 2.41	14.88 ± 3.25	13.35 ± 2.52
f_1-f_5-f_6-f_4-f_3-f_2	0.62 ± 0.80	**3.05 ± 1.51**	**11.71 ± 3.18**	**9.88 ± 2.28**

The results in Table 1 indicate the best classification performance for usage of all the features together. The best separation ability has been achieved between classes C – B representing control group and RNFL defects, respectively. It means the RNFL loss can be quite well distinguished from the RNFL tissue of healthy patients with the average classification error of 0.55%. The classification error between classes A – B is worse, but still well performed (3.05%). This is probably caused by lower appearance of the RNFL striation in class A due to the glaucoma progression in the eyes affected by glaucoma. The higher classification error was achieved for classes A – C (11.71%); both classes contain RNFL texture. Nevertheless, this still relatively low error proves that separation of the RNFL into the three defined classes is reasonable.

Using three-state classifier allows us to distinguish the classes from each other (last column in Table 1) with classification error of 9.88%. This value represents the classification error when we analyze the whole fundus image. In this task we try to classify the RNFL defects (class B) and also the changes in RNFL striation due to glaucoma progression (classes A and C).

4.2 RNFL loss detection

Supervised three-state machine learning via Bayesian classifier using labelled training dataset (image regions in classes A, B and C) was applied on the input fundus-camera image.

The testing of input retinal image was performed in the rectangular region of interest (ROI) corresponding to the diagnostically most important area around the ONH automatically allocated using our previously developed ONH detection approach [11]. This method uses simple intensity criterion and Hough transform to detect the center of ONH and active contours for ONH segmentation.

The blood vessels need to be masked out so that the texture would be analyzed only in the non-vessels area. The vessels were segmented by our algorithm recently presented in [7]. This approach is based on the matched filters with 2D impulse responses obtained via averaging of brightness profiles of vessels for five different vessel widths. Each of the basic masks was rotated in twelve different directions, which gives finally a number of 60 masks of the matched filters.

A small square pixel neighborhood of the same size as above described image regions (97 × 97 pixels) was scanned

within the non-vessels area of the original image in the ROI pixel-by-pixel and the three-state supervised classification was performed.

A fundus-camera image with distinctive RNFL loss of glaucomatous patient in our retinal image database was chosen for the analysis. The results of RNFL loss detection are presented in Figure 4a. Three colours within the ROI represent three-state output of the classifier: red – class B (RNFL loss) yellow – class A (healthy tissue of patient with glaucoma), green – class C (healthy tissue of patient without glaucoma). The analyzed image was subjectively compared with the RNFL loss marked by experienced ophthalmologist. The result shows that the red area was marked correctly. It means that the RNFL defect can be detected by the proposed approach (Figure 4a).

The RNFL in image of healthy patient without glaucoma has been also analyzed within the ROI (Figure 4b). The output indicates much more green labelled area as we assumed than in the previous case of glaucomatous eye. The yellow labelled regions could be hypothetically interpreted as RNFL tissue possibly suspected of glaucoma, but this is probably influenced by the mentioned classification error. However, the RNFL detection is also probably influenced by the artefacts due to incorrect blood vessels masking or due to specific physiological or pathological structures, which might be occurred in the examined eye and they negatively influence retinal image acquisition.

4.3 Comparison with OCT measurements

The OCT imaging provides cross-sectional images (B–scans) of the retina, which makes it possible to quantitatively measure the RNFL thickness. Therefore, the OCT image can be regarded as a gold standard for our application allowing a comparison with proposed RNFL detection in colour fundus images. An example of such a B–scan with clearly marked RNFL loss by experienced ophthalmologist is shown in Figure 5b. The result of proposed automated RNFL loss detection using fundus-camera image of the same patient with depiction of cross-sectional B–scan position is illustrated in Figure 5a. It can be clearly seen that the RNFL losses correspond quite well.

The RNFL thickness measurement using B-scans is commercially available and provided by a range of algorithms, e.g. [3, 8, 12]. A comparison of RNFL analysis in fundus images with such a RNFL thickness measurement via OCT offers an idea of RNFL thickness mapping in fundus image. However, this will be largely dependent on the resolution and quality of fundus-camera images taken. We just have only 3 classes of RNFL thickness belonging to the colours in Figure 5a. The highest thickness of the RNFL belongs to green; mediate RNFL thickness (suspected of glaucoma) is represented by yellow and the RNFL losses with zero thickness by red colour, respectively.

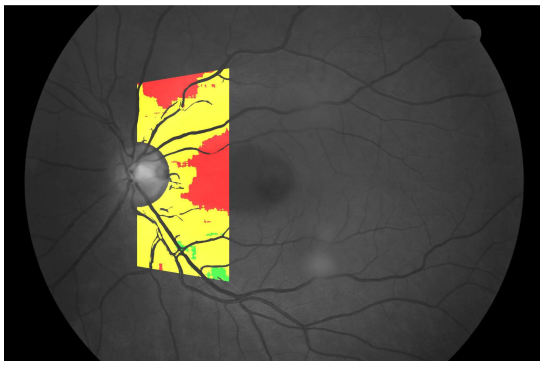

a)

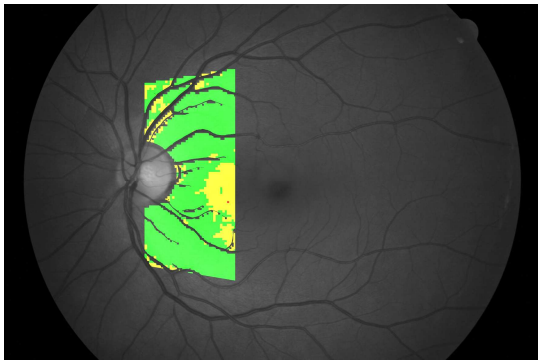

b)

Figure 4 – Results of RNFL detection; a) left eye of a glaucomatous patient with distinctive RNFL loss, b) left eye of a healthy patient without any glaucoma defects.

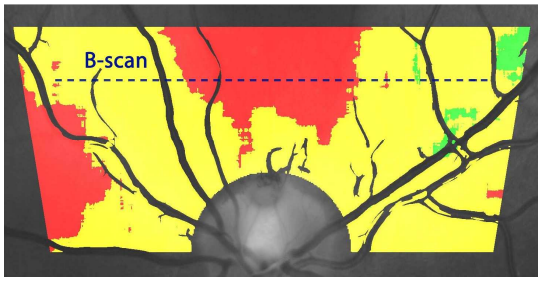

a)

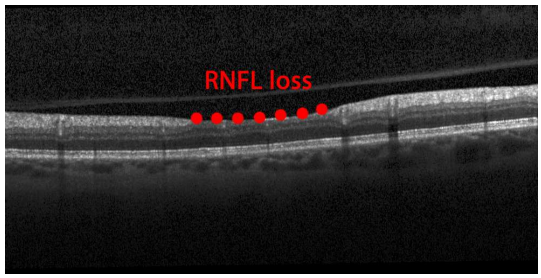

b)

Figure 5 – RNFL loss detection comparing with the OCT B-scan; a) Depiction of a B-scan position in rotated section of fundus-camera image from Figure 4a, b) Example of OCT cross–sectional B-scan of the same patient with RNFL loss as in case of a).

5. CONCLUSIONS

The Gaussian Markov random field texture analysis method was presented aimed to model the RNFL texture. The results indicate that the proposed GMRF features can be quite successfully used for discrimination between healthy and glaucomatous RNFL tissue in connection with the supervised machine learning approach based on the non-linear Bayesian classifier. The classification performance was quantitatively evaluated by repeated random sub-sampling cross-validation method with relatively good accuracy – the classification error reaches only 0.55% discriminating the image regions of classes C – B and 3.05% of classes A – B, respectively. Discrimination ability between classes A and C is worse with an error of 11.71%; the both classes appear similar with the RNFL texture, although one is probably influenced by progression of the disease. As well, the classification errors were probably caused by the clusters overlapping in the feature space, because a strong separating hyperplane between the particular classes does not exist.

The three-state supervised classifier was tested within the diagnostically important area in the fundus-camera image of patient with glaucoma. The classification results were compared with OCT measurements showing a relatively good correlation between the RNFL changes. This result suggests the possibility of RNFL thickness mapping according to the disease progression in further research.

ACKNOWLEDGEMENT

This work has been supported by the national research center DAR (Data, Algorithms and Decision making) project no. 1M0572 coordinated by the Institute of Information Theory and Automation, Academy of Science, Czech Rep. and partly also by the institutional research frame no. MSM 0021630513; both grants sponsored by the Ministry of Education of the Czech Republic. The authors highly acknowledge the cooperation with the Eye Clinic Zlin, Czech Rep. (T. Kubena, M.D. and P. Černošek, MSc), through which also the test set of images was provided.

REFERENCES

[1] A. Tuulonen et al., "Digital imaging and microtexture analysis of the nerve fibre layer," *Journal of Glaucoma*, vol. 9, pp. 5–9, 2000.

[2] A M. Oliva, D. Richards, W. Saxon, "Search for Color-Dependent Nerve-Fiber-Layer Thinning in Glaucoma: A Pilot Study," *ARVO 2007*, May 6-10, 2007, Fort Lauderdale, USA, E-Abstract 3309.

[3] D. Koozekanani, et al., " Retinal thickness measurement from optical coherence tomography using a Markov boundary model," *IEEE Transaction on Medical Imaging*, vol. 20(9), pp. 900-916, Sept. 2001.

[4] E. Peli, T R. Hedges, B, Schwartz, "Computer measurement of the retina nerve fiber layer striations," *Applied Optics*, vol. 28, pp. 1128–1134, 1989.

[5] H. Peng, F. Long, Ch. Ding, "Feature selection based on mutual information: Criteria of max dependency, max-relevance and min-redundancy," *IEEE Trans. on Patt. Analys. and Mach. Intel*, vol.27(8), pp. 1226-1238.

[6] J. Gazárek, J. Jan, R. Kolář, "Detection of Neural Fibre Layer in Retinal Images via Textural Analysis," in *Proc. BIOSIGNAL'08*, Brno, Czech Rep., June 2008, CD issue.

[7] J. Odstrčilík, J. Jan, R. Kolář, J. Gazárek, "Improvement of Vessel Segmentation by Matched Filtering in Colour Retinal Images," in *Proc. of World Congress on Medical Physics and Biomedical Engineering*, Munich, Germany, Sept. 2009, pp. 327-330.

[8] L. Zongging et al., "A variational approach to automatic segmentation of RNFL on OCT data sets of the retina," *16th IEEE International Conference on image processing (ICIP)*, Cairo, Egypt, Nov. 2009, pp. 3345-3348.

[9] M.T. Dardjat, et al., "Application of Image Processing Technique for Early Diagnosis and Monitoring of Glaucoma," in *Proc. KOMMIT 2004*, Jakarta, Aug.24-25, 2004, pp. 238-245.

[10] M. Lundström, O J. Eklundh, "Computer Densitometry of Retinal Nerve Fibre Atrophy – a pilot study," *Acta Ophthalmologica*, vol. 58, No. 4, pp. 639-644, 1980.

[11] M. Malínský, R. Kolář, J. Jan, "Localization of the optic nerve head in colour fundus images," in *Proc. BIOSIGNAL'08*, Brno, Czech Rep., June 2008, CD issue.

[12] M. Shahidi, et al., "Quantitative thickness measurement of retinal layers imaged by optical coherence tomography," *Am J. Ophthalmol*, vol. 139, pp. 1056–1061, June 2005.

[13] P. Paalanen, J. Kamarainen, J. IIonen, H. Kalviainen, „Feature representation and discrimination based on Gaussian mixture model probability densities—Practices and algorithms," *Pattern Recognition*, vol. 39(7), pp. 1346-1358, 2006.

[14] R. Ansari et al., "A method for detection of retinal layers by optical coherence tomography image segmentation," *Life Science Systems and Applications Workshop*, LISA Nov. 2007, pp. 144-147.

[15] R. Bock, J. Meier, G. Michelson, L G. Nyul, J. Hornegger, "Classifying glaucoma with image-based features from fundus photographs," *Lecture Notes in Computer Science, Springer*, vol. 4713, pp. 355 – 365, 2007.

[16] R. Kolář, D. Urbánek, J. Jan, "Texture based discrimination of normal and glaucomatous retina," in *Proc. BIOSIGNAL'08*, Brno, Czech Rep., June 2008, CD issue.

[17] R. Kolář, J. Jan, "Detection of glaucomatous eye via color fundus images using fractal dimensions," *Radioengineering*, vol. 17(3), pp. 109-114, Nov. 2008.

[18] R. Porter, N. Canagarajah, "Robust rotation-invariant texture classification: wavelet, Gabor filter and GMRF based schemes," *IEEE Proc. Vis.-Image Signal Processing*, vol. 144(3), pp. 180-188, 1997.

[19] R P. Tornow, R. Laemmer, Ch. Mardin, "Quantitative Imaging Using a Fundus Camera," *ARVO 2007, May 6-10, 2007*, Fort Lauderdale, USA, e-abstract 1206.

[20] S. Z. Li, *Markov Radnom Field Modeling in Image Analysis*. Springer, 2009.